Article

Elongation of Ordered Peptide Aggregate of an Amyloidogenic Hexapeptide NFGAIL Observed in Molecular Dynamics Simulations with Explicit Solvent

Chun Wu, Hongxing Lei, and Yong Duan

J. Am. Chem. Soc., **2005**, 127 (39), 13530-13537• DOI: 10.1021/ja050767x • Publication Date (Web): 08 September 2005

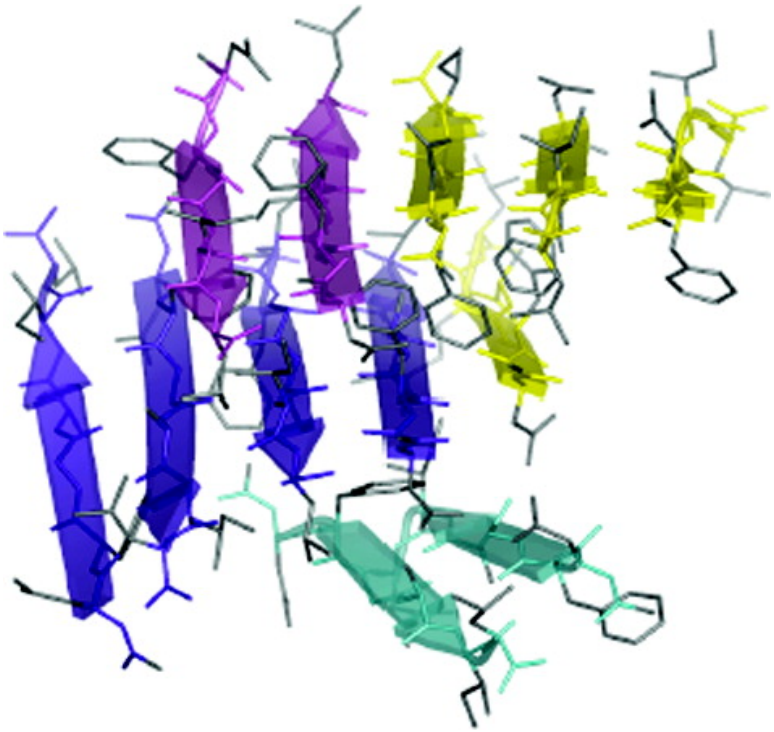

J|A|C|S
ARTICLES
Published on Web 09/08/2005

Elongation of Ordered Peptide Aggregate of an Amyloidogenic Hexapeptide NFGAIL Observed in Molecular Dynamics Simulations with Explicit Solvent

Chun Wu,[†,‡] Hongxing Lei,[‡] and Yong Duan*[,‡]

Contribution from the Department of Chemistry and Biochemistry, University of Delaware, Newark, Delaware 19716, and UC Davis Genome Center and Department of Applied Science, University of California, Davis, California 95616

Received February 4, 2005; E-mail: duan@ucdavis.edu

Abstract: The mechanisms by which amyloidogenic peptides and proteins form soluble toxic oligomers remain elusive. We have studied the formation of partially ordered tetramers and well-ordered octamers of an amyloidogenic hexapeptide NFGAIL (residues 22−27 of the human islet amyloid polypeptide) in our previous work. Continuing the effort, we here probe the β-sheet elongation process by a combined total of 2.0 μs molecular dynamics simulations with explicit solvent. In a set of 10 simulations with the peptides restrained to the extended conformation, we observed that the main growth mode was elongation along the β-sheet hydrogen bonds through primarily a two-stage process. Driven by hydrophobic forces, the peptides initially attached to the surface of the ordered oligomer, moved quickly to the β-sheet edges, and formed stable β-sheet hydrogen bonds. Addition of peptides to the existing oligomer notably improved the order of the peptide aggregate in which labile outer layer β-sheets were stabilized, which provides good templates for further elongation. These simulations suggested that elongation along the β-sheet hydrogen bonds occurs at the intermediate stage when low-weight oligomers start to form. We did not observe significant preference toward either parallel or antiparallel β-sheets at the elongation stage for this peptide. In another set of 10 unrestrained simulations, the dominant growth mode was disordered aggregation. Taken together, these results offered a glimpse at the molecular events leading to the formation of ordered and disordered low-weight oligomers.

Introduction

Amyloidogenesis is an important biophysical process that has been associated with a number of human diseases including Alzheimer's disease, type II diabetes, prion disease, Parkinson's, and Huntington's diseases.[1−4] In these processes, proteins or peptides are associated together to form toxic soluble oligomers[5,6] and subsequently insoluble amyloid fibrils. Although amyloidogenic proteins or peptides do not share any sequence homology or common structure, the amyloid oligomers/fibrils share a general "cross-β" structure,[7−9] underscoring the similarity of the underlying physical mechanisms.[6,10] Although tremendous effort and progress have been made, including the advent of anti-amyloid agents,[11−13] the early stage formation of the soluble oligomers and subsequent elongation processes remain poorly understood.

In the aggregation process, peptides are thought to form low-weight soluble oligomers first. These early oligomeric species are thought to be toxic,[5,10,14] eventually growing to form highly ordered insoluble amyloid fibrils. Despite the key clinical significance, little is known about the structures of the early soluble toxic oligomeric species[5] formed by the amyloidogenic peptides and proteins, and even less is known about the underlying physical mechanisms and the dynamic process by which these species form. These are two of the key issues that need to be addressed for a comprehensive understanding of the mechanisms of amyloidogenesis, which would help the design of more effective therapeutic strategies.

In addition to the extensive experimental studies, numerous computational studies have also been performed. Various

[†] University of Delaware.
[‡] University of California.

(1) Thirumalai, D.; Klimov, D. K.; Dima, R. I. *Curr. Opin. Struct. Biol.* **2003**, *13*, 146−159.
(2) Rochet, J. C.; Lansbury, P. T. *Curr. Opin. Struct. Biol.* **2000**, *10*, 60−68.
(3) Dobson, C. M. *Trends Biochem. Sci.* **1999**, *24*, 329−332.
(4) Kelly, J. W. *Curr. Opin. Struct. Biol.* **1998**, *8*, 101−106.
(5) Hardy, J.; Selkoe, D. J. *Science* **2002**, *297*, 353−356.
(6) Kayed, R.; Head, E.; Thompson, J. L.; McIntire, T. M.; Milton, S. C.; Cotman, C. W.; Glabe, C. G. *Science* **2003**, *300*, 486−489.
(7) Jaroniec, C. P.; MacPhee, C. E.; Bajaj, V. S.; McMahon, M. T.; Dobson, C. M.; Griffin, R. G. *Proc. Natl. Acad. Sci. U.S.A.* **2004**, *101*, 711−716.
(8) Sunde, M.; Serpell, L. C.; Bartlam, M.; Fraser, P. E.; Pepys, M. B.; Blake, C. C. F. *J. Mol. Biol.* **1997**, *273*, 729−739.
(9) de la Paz, M. L.; Goldie, K.; Zurdo, J.; Lacroix, E.; Dobson, C. M.; Hoenger, A.; Serrano, L. *Proc. Natl. Acad. Sci. U.S.A.* **2002**, *99*, 16052−16057.
(10) Bucciantini, M.; Calloni, G.; Chiti, F.; Formigli, L.; Nosi, D.; Dobson, C. M.; Stefani, M. *J. Biol. Chem.* **2004**, *279*, 31374−31382.
(11) Blanchard, B. J.; Chen, A.; Rozeboom, L. M.; Stafford, K. A.; Weigele, P.; Ingram, V. M. *Proc. Natl. Acad. Sci. U.S.A.* **2004**, *101*, 14326−14332.
(12) Mason, J. M.; Kokkoni, N.; Stott, K.; Doig, A. J. *Curr. Opin. Struct. Biol.* **2003**, *13*, 526−532.
(13) Gestwicki, J. E.; Crabtree, G. R.; Graef, I. A. *Science* **2004**, *306*, 865−869.
(14) Bucciantini, M.; Giannoni, E.; Chiti, F.; Baroni, F.; Formigli, L.; Zurdo, J. S.; Taddei, N.; Ramponi, G.; Dobson, C. M.; Stefani, M. *Nature* **2002**, *416*, 507−511.

10.1021/ja050767x CCC: $30.25

simplified models have been used to sample the self-assembly pathways of KFFE hexamers,[15] to study oligomerization of amyloid A-beta (16−22) peptides,[16−18] to probe the general properties of protein and peptide aggregation,[19] to search possible aggregating conformations of SH3 domain,[20] to study the competition between protein folding and aggregation of a tetrameric β-sheet complex,[21] and to investigate spontaneous fibril formation by random-coil peptides.[22] All-atom molecular dynamics (MD) simulations have been applied to study amyloid fibril stability.[23−25] Early stage aggregation has also been studied with the assistance of inter-strand harmonic restraining forces [26,27] to accelerate the aggregation process. Recently, all-atom molecular dynamics with a continuum solvent model was used to study dimer formation of amyloidogenic peptides,[28] amyloid aggregation of multiple peptide fragment of transthyretin,[29] and conformational transition of the prefibrillar amyloidogenic intermediate.[30]

The islet amyloid polypeptide, a 37-amino acid hormone, is the main constituent of the islet amyloid fibrils found in 95% of type II diabetes mellitus.[31,32] It has been established that IAPP forms amyloid fibrils[33] in vitro, which induces islet cell apoptosis.[34] The peptide NFGAIL, a fragment truncated from human IAPP (residues 22−27), is one of the shortest fragments that have been shown to form amyloid fibrils similar to those formed by the full polypeptide.[35] Furthermore, the fibrils formed by the hexapeptide were also cytotoxic toward the pancreatic cell line. Thus, the short NFGAIL fragment is a good model system to study the formation of the amyloid fibril and its cytotoxicity.

In a series of studies on the formation of ordered aggregates of hexapeptide NFGAIL, we employed all-atom molecular dynamics simulations with explicit solvent and particle-mesh Ewald method for the treatment of long-range electrostatic forces.[36] Although the approach is computationally expensive in comparison to continuum solvent models, it is perhaps the only method that can reveal detailed atomic level information of the solvation and the role of solvent that would in turn help to enhance our understanding of the underlying physical mechanisms. This is important in the studies of amyloidosis because one important question concerns the formation of inter-strand main-chain hydrogen bonds and their roles in oligomerization. Thus, an accurate representation of both peptide and water hydrogen-bond groups is necessary.

In our first study,[37] formation of the partially ordered tetramers of the peptide NFGAIL was observed in the simulations. In our second study,[38] formation of well-ordered octamers of the peptide was observed by using two-strand β-sheets as subunits for the association simulations. In this ordered oligomer, eight peptides organized into a three-layer β-sheet structure with a four-strand β-sheet as the middle layer. We now take a step further to study elongation of this ordered peptide oligomer.

In this study, four monomeric peptides were placed in the water box with the preformed ordered peptide oligomer reported in our previous study.[38] Two sets of simulations were conducted. In one set, the peptide main chains were restrained to the extended conformation to accelerate the elongation process. In the second set of simulations, the conformational restraints were removed.

Method

Systems. Four NFGAIL peptide monomers and a preformed octamer ordered peptide aggregate[38] were immersed into a triclinic box of 7093 water molecules, equivalent to a truncated-octahedral box. The entire system has a total of 22 419 atoms. The final box dimensions were $a = b = c = 66.84$ Å, $\alpha = \beta = \gamma = 109.47°$. The four peptides were initially placed perpendicular to the β-sheet planes of the octamer ordered peptide aggregate. They were also separated from the octamer by about 20 Å of water (e.g., Figure 2A, water not shown). The monomer and the octamer concentrations were ∼29 and ∼7 mM, respectively. In the first set of 10 simulations, the peptides were restrained to the β-extended conformation by restraining the main-chain torsion angles around ($\Phi \approx -110°$, $\Psi \approx 135°$) throughout the simulations. In the second set of 10 simulations, no conformational restraints were imposed on the peptides.

MD Simulation. The AMBER simulation package was used in both molecular dynamics simulations and data processing.[39] The Duan et al. all-atom point-charge force field[40] was chosen to represent the peptide, and the N and C termini were blocked, respectively, by acetyl and amine groups. The solvent was explicitly represented by the TIP3P water model. The peptide−water systems were subjected to periodic boundary conditions via both minimum image and Discrete Fourier Transform as part of the particle-mesh Ewald method.[36] After the initial energy minimization, 10 simulations for each set were carried out for a peptide−water system. These 10 simulations started from the same coordinates but with different initial random velocities by choosing different random number seeds. The initial velocities were generated according to the Boltzmann's distribution at 500 K. The simulations started from a 10.0 ps run at 500 K to randomize the orientations and positions of the four peptides. The systems were then subjected to 1 ns at 320 K in the NPT ensemble (constant number of atoms in the box, constant pressure, and temperature) to adjust system size and density, and to fully solvate the peptides. The simulations were continued at 320 K for 99 ns in the NVT ensemble (constant number

(15) Wei, G. H.; Mousseau, N.; Derreumaux, P. *Biophys. J.* **2004**, *87*, 3648−3656.
(16) Favrin, G.; Irback, A.; Mohanty, S. *Biophys. J.* **2004**, *87*, 3657−3664.
(17) Santini, S.; Mousseau, N.; Derreumaux, P. *J. Am. Chem. Soc.* **2004**, *126*, 11509−11516.
(18) Santini, S.; Wei, G. H.; Mousseau, N.; Derreumaux, P. *Structure* **2004**, *12*, 1245−1255.
(19) Dima, R. I.; Thirumalai, D. *Protein Sci.* **2002**, *11*, 1036−1049.
(20) Ding, F.; Dokholyan, N. V.; Buldyrev, S. V.; Stanley, H. E.; Shakhnovich, E. I. *J. Mol. Biol.* **2002**, *324*, 851−857.
(21) Jang, H. B.; Hall, C. K.; Zhou, Y. Q. *Biophys. J.* **2004**, *86*, 31−49.
(22) Nguyen, H. D.; Hall, C. K. *Proc. Natl. Acad. Sci. U.S.A.* **2004**, *101*, 16180−16185.
(23) Li, L. P.; Darden, T. A.; Bartolotti, L.; Kominos, D.; Pedersen, L. G. *Biophys. J.* **1999**, *76*, 2871−2878.
(24) Zanuy, D.; Ma, B. Y.; Nussinov, R. *Biophys. J.* **2003**, *84*, 1884−1894.
(25) Zanuy, D.; Nussinov, R. *J. Mol. Biol.* **2003**, *329*, 565−584.
(26) Gsponer, J.; Haberthur, U.; Caflisch, A. *Proc. Natl. Acad. Sci. U.S.A.* **2003**, *100*, 5154−5159.
(27) Klimov, D. K.; Thirumalai, D. *Structure* **2003**, *11*, 295−307.
(28) Hwang, W.; Zhang, S. G.; Kamm, R. D.; Karplus, M. *Proc. Natl. Acad. Sci. U.S.A.* **2004**, *101*, 12916−12921.
(29) Paci, E.; Gsponer, J.; Salvatella, X.; Vendruscolo, M. *J. Mol. Biol.* **2004**, *340*, 555−569.
(30) Armen, R. S.; DeMarco, M. L.; Alonso, D. O. V.; Daggett, V. *Proc. Natl. Acad. Sci. U.S.A.* **2004**, *101*, 11622−11627.
(31) Westermark, P.; Wernstedt, C.; Obrien, T. D.; Hayden, D. W.; Johnson, K. H. *Am. J. Pathol.* **1987**, *127*, 414−417.
(32) Hoppener, J. W. M.; Ahren, B.; Lips, C. J. M. *New Engl. J. Med.* **2000**, *343*, 411−419.
(33) Makin, O. S.; Serpell, L. C. *J. Mol. Biol.* **2004**, *335*, 1279−1288.
(34) Lorenzo, A.; Razzaboni, B.; Weir, G. C.; Yankner, B. A. *Nature* **1994**, *368*, 756−760.
(35) Tenidis, K.; Waldner, M.; Bernhagen, J.; Fischle, W.; Bergmann, M.; Weber, M.; Merkle, M. L.; Voelter, W.; Brunner, H.; Kapurniotu, A. *J. Mol. Biol.* **2000**, *295*, 1055−1071.
(36) Essmann, U.; Perera, L.; Berkowitz, M. L.; Darden, T. A.; Lee, H.; Pedersen, L. G. *J. Chem. Phys.* **1995**, *103*, 8577−8593.
(37) Wu, C.; Lei, H.; Duan, Y. *Biophys. J.* **2004**, *87*, 3000−3009.
(38) Wu, C.; Lei, H.; Duan, Y. *Biophys. J.* **2005**, *88*, 2897−2906.
(39) Case, D. A.; et al. University of California: San Francisco, 2002.
(40) Duan, Y.; Chowdhury, S.; Xiong, G.; Wu, C.; Zhang, W.; Lee, T.; Cieplak, P.; Caldwell, J.; Luo, R.; Wang, J.; Kollman, P. A. *J. Comput. Chem.* **2003**, *24*, 1999−2012.

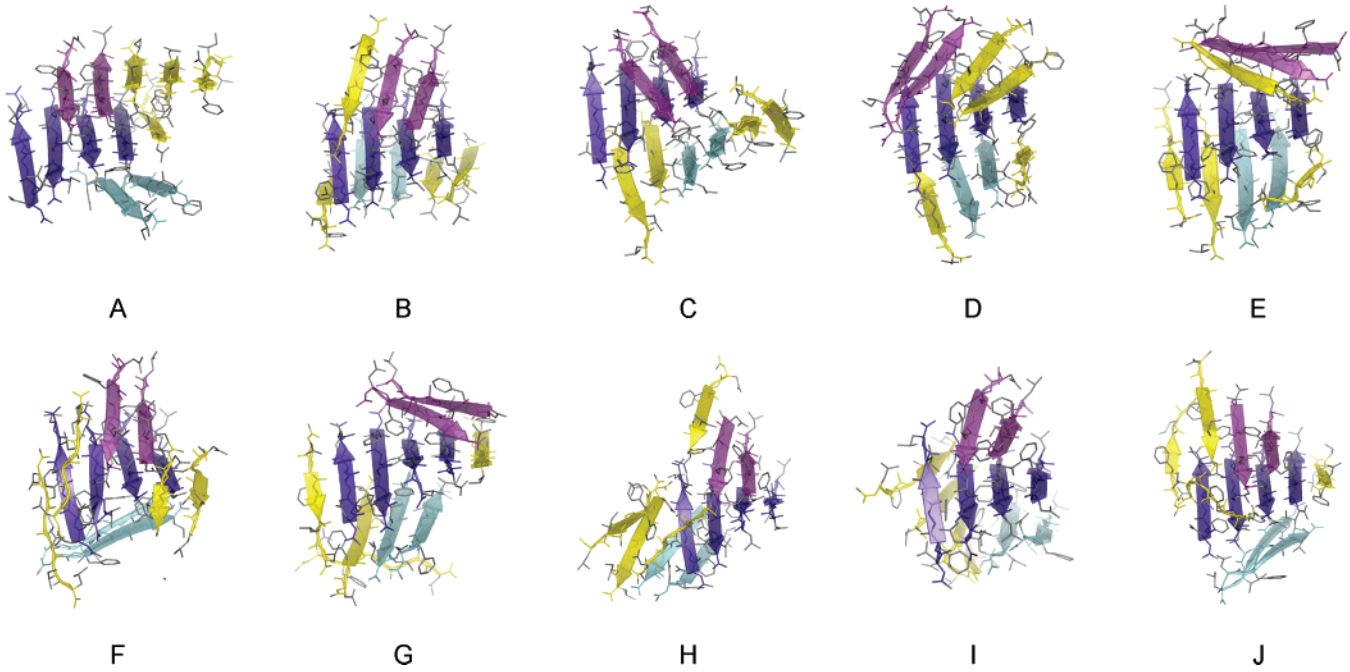

Figure 1. The final snapshots from the 10 restrained simulations. The three layers of the initial ordered peptide aggregate are in purple (upper), wheat (middle), and cyan (bottom), respectively. The yellow peptides were added at the beginning of the simulations as monomer peptides and became part of the peptide aggregate during the simulations. For clarity, water molecules are not shown.

of atoms in the box, constant volume, and constant temperature). Particle-mesh Ewald method[36] was used to treat the long-range electrostatic interactions. SHAKE[41] was applied to constrain all bonds connecting hydrogen atoms, and a time step of 2.0 fs was used. To reduce the computation, nonbonded forces were calculated using a two-stage RESPA approach[42] where the forces within a 10 Å radius were updated every step and those beyond 10 Å were updated every two steps. Temperature was controlled at 320 K by using Berendsen's algorithm[43] with a coupling constant of 2.0 ps. The center of mass translation and rotation were removed every 100 steps. Studies have shown this removes the "block of ice" problem.[44,45] The trajectories were saved at 10 ps intervals, and 100 000 snapshots from each set of simulations were produced for further analyses.

Results

In the following discussion, we refer to the aggregate of multiple peptides (sequence NFGAIL) as "peptide aggregate", which may include both ordered and nonordered forms. In the ordered form (or ordered peptide aggregate), the peptides form multilayer β-sheets and are aligned in either parallel or antiparallel orientations. The nonordered form may include the partially ordered aggregate of mixed ordered and disordered peptides. We refer to the peptides that are not part of an aggregate as peptide monomers or monomeric peptides. We will first discuss the observations made from the set of 10 restrained simulations and then discuss the results from a set of 10 unrestrained simulations.

Starting from a nucleus of eight-peptide ordered aggregate in three-layer β-sheet configuration as reported in our earlier study,[38] four additional monomeric peptides were placed 20 Å away from the nucleus. In the first set of 10 simulations (100 ns each), each peptide was restrained to the extended conformation. The initial ordered aggregate showed remarkable stability, and its structure was very well maintained in all 10 simulations and the relative alignment between the layers was also improved. At the end of 100 ns, free monomers were orderly attached to the aggregate. Three-layer ordered oligomers were produced in seven simulations whereby the β-sheets were extended along the hydrogen bonds. Four-layer ordered aggregates were also produced in two simulations (Figure 1H and I). Thus, elongation along the β-sheet hydrogen-bond direction was a preferred mode of growth, and the initial three-layer β-sheet architecture of the octamer was well maintained in majority of the simulations.

For clarity, the snapshots in Figure 1 are shown in similar orientation. Among the three layers of the initial ordered octamer, as shown in Figure 2 (center of 0.0 ns), the middle layer was a four-strand β-sheet and both the upper and the lower layers were two-strand β-sheets. The upper layer β-sheet was in parallel/antiparallel to the central layer. The lower layer β-sheet was rotated by almost 90° relative to the central layer along the normal axis of its β-sheet plane and was almost orthogonal to both the upper and the central layers (the original structure of the initial peptide octamer can be seen in Figure 2 at 0.0 ns).

During the simulations, the initial four strands of the central layer β-sheet stayed together and remained as a four-strand β-sheet in all simulations. The central layer grew to five strands in two trajectories and to six strands in the two other trajectories. The upper layer two-strand β-sheet, which was initially in an ordered β-sheet alignment parallel/antiparallel to the central layer, grew to five strands in one trajectory, to four strands in another trajectory, and three strands in four trajectories. On average, each of the upper and middle layers grew by one strand, and the lower layer grew by 1.5 strands.

(41) Ryckaert, J.-P.; Ciccotti, G.; Berendsen, H. J. C. *J. Comput. Phys.* **1977**, *23*, 327−341.
(42) Procacci, P.; Berne, B. J. *Mol. Phys.* **1994**, *83*, 255−272.
(43) Berendsen, H. J. C.; Postma, J. P. M.; van Gunsteren, W. F.; DiNola, A.; Haak, J. R. *J. Comput. Phys.* **1984**, *81*, 3684−3690.
(44) Chiu, S. W.; Clark, M.; Subramaniam, S.; Jakobsson, E. *J. Comput. Chem.* **2000**, *21*, 121−131.
(45) Harvey, S. C.; Tan, R. K. Z.; Cheatham, T. E. *J. Comput. Chem.* **1998**, *19*, 726−740.

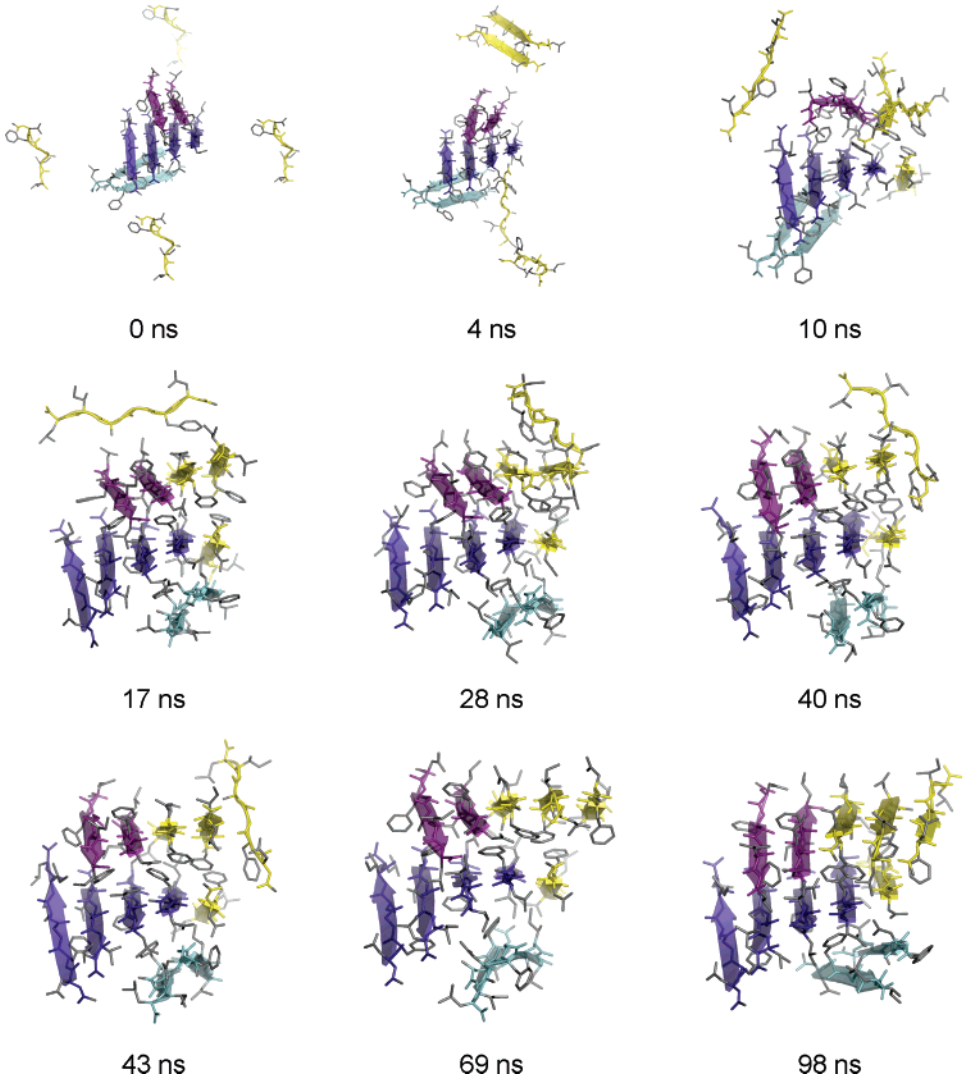

Figure 2. Snapshots from a representative trajectory. The three layers of the initial ordered peptide octamer are in purple (upper), wheat (middle), and cyan (bottom), respectively. The yellow peptides were initially placed 20 Å away from the ordered peptide aggregate. For clarity, water molecules are not shown.

Although there was no clear tendency to attach to any of the three layers, the attachment of new strands appears to influence the alignment of the outer layers. In particular, when new strands were attached to the lower layer, which was initially almost orthogonal to the central layer, the same layer rotated relative to the central layer along the normal axis of its β-sheet plane and became almost parallel/antiparallel to the central layer. In contrast, it remained close to its initial orientation in three of the four cases where no new strands were attached to the lower layer. This indicated that, where this layer may rotate easily within the β-sheet plane in the absence of new strands, addition of new strands could stabilize it toward the ordered parallel/antiparallel orientation. Thus, elongation makes the layers better aligned and the peptide aggregate more ordered. This is an important step toward the stable ordered peptide aggregate because addition of new strands stabilizes ordered structure and makes it easier to elongate further.

Judging from the fact that most four-strand β-sheets were well-aligned against other layers, it appears that the four-strand β-sheets are sufficient to provide stable template for further elongation of the fibrillar ordered peptide aggregate when they are stacked in multilayer. Conversely, the two-strand β-sheets were often aligned poorly with respect to other layers. Because correction of the alignment is needed for ordered growth, the poor alignment may hinder the propagation of the layer. Therefore, two-strand β-sheets of short peptides alone appear insufficient to be the starting templates of further growth, and their orientation may need to be stabilized by additional peptides. For longer peptides and other hexapeptides, however, stable two-strand β-sheets may form, from which further growth may be possible.

We observed two elongation pathways. The dominant pathway was the attachment to the ordered peptide aggregate one peptide monomer at a time. Alternatively, we also observed in four of the 10 simulations that some peptide monomers associated with each other to form dimers and then attached to the ordered peptide aggregate. The latter pathway was probably enhanced by the elevated concentration of the peptide monomer added to the system in the simulations. With the present setup, the effective concentration of the monomeric peptides started at $\sim$29 mM, which is substantially higher than the peptide concentration at the physiological condition. Because dimer concentration is proportional to the square of monomer concentration, peptide dimers are expected to be less stable at the physiological peptide concentration. Thus, we anticipate that the first pathway may be prevalent in which the ordered peptide

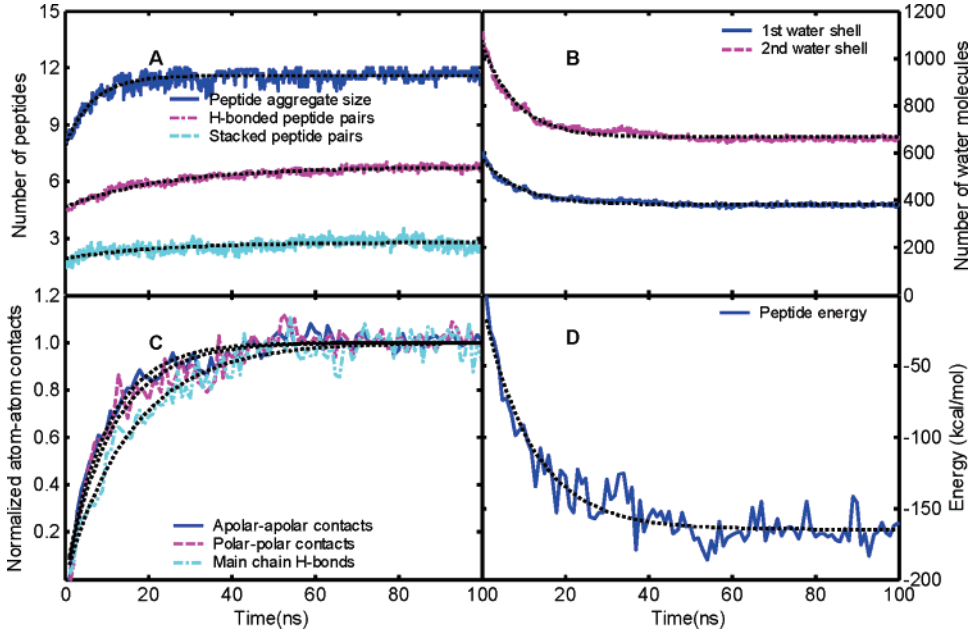

Figure 3. Properties of the peptides averaged over the simulations. All curves are fitted by $A \exp(-t/T) + B$, and the fitting parameters are tabulated in Table 1. (A) Size of peptide aggregate (blue); number of peptides in hydrogen-bonded peptide pairs (magenta); number of peptides in the stacked pairs (cyan). (B) Number of water molecules in the first (0.0−3.4 Å) and second (3.4−5.0 Å) solvation shells of the peptides. (C) Inter-strand apolar−apolar (blue), polar−polar (magenta) contacts, and hydrogen bonds (cyan). For clarity, the contacts were minimized and scaled by $(y - (A + B))/A$ such that the starting value is 0 and the equilibrium value is 1.0. Two atoms were considered in contact when their distance was closer than their VDW radii plus 2.8 Å. Hydrogen bonds were counted when the heavy atom distances was less than 4.0 Å and the O:HN angle is greater than 120°. (D) Total potential energy of the peptides.

aggregate grows by adding one peptide at a time. Addition of dimers should be possible, because the relaxation time of dimers was estimated to be longer than the time for diffusional encounters with other oligomers.[28] However, it should be a secondary pathway because the peptide dimers are expected to be less stable at lower concentration.[37]

Snapshots from a representative trajectory are shown in Figure 2. In this trajectory, two free peptide monomers started to form a dimer at around 4.0 ns. In the meantime, another free peptide monomer started to aggregate to ordered octamer. At this point, however, the growth mode was mostly disordered that the newly attached peptide did not form a β-sheet. At 10 ns, the first attached monomer moved to the middle layer and extended the β-sheet along its main-chain hydrogen-bond direction. This marked the first elongation of the β-sheet and ordered growth of the aggregate. At 17 ns, the peptide dimer also formed ordered β-sheet extension to the upper layer. The remaining peptide monomer initially attached to the ordered peptide aggregate in a disordered mode and moved gradually to the upper layer and extended the ordered β-sheet at 43 ns, which completed the elongation. This new three-layer β-sheet structure was stable throughout the rest of the 100 ns simulation.

Although the exact sequence and time of the events varied from one trajectory to another, most of the events described above were observed in multiple trajectories. We observed the formation of isolated dimer in four trajectories. Other common observations included attachment of monomers to the aggregate directly as observed initially in the random positions, and then they subsequently moved to elongate the β-sheets. Therefore, the trajectory described above represents a typical snapshot of the events leading to the formation of ordered low-weight oligomers in the early stage.

The oligomeric state of the peptide aggregate was monitored by counting the number of peptides. The size of the peptide aggregate was averaged over the simulations and is shown in Figure 3A (blue line). We also fitted the curve by an exponential function $A \exp(-t/T) + B$, and the fitting parameters are given in Table 1. Overall, the development of peptide aggregate size can be represented well by a single exponential function, suggesting a first-order growth process, consistent with the notion that the peptide aggregate grows by adding one peptide at a time. The time constant was 6.6 ns, which was notably faster than the formation of ordered peptide aggregate as measured by both hydrogen-bonded pairs and the orderly stacked pairs shown in Figure 3A in magenta and cyan lines. The time constant of ordered peptide aggregate formation was about 22.0−23.0 ns, 3 times more slowly than peptide aggregate. Thus, one can clearly identify a two-stage process. In the first stage, peptides aggregated to the existing ordered peptide aggregate. They then moved to form ordered aggregate. This was similar to the zipper-like mechanisms observed by Hwang et al. on other peptides.[28] Interestingly, because of the single-exponential growth, it appears that the dissociation process was not needed to re-align the peptides. This was different than what we observed in our earlier study in which peptide aggregates underwent constant breaking and formation,[37] suggesting that

Table 1. Fitting Parameters of the Curves in Figure 3[a]

	T (ns)	A	B
peptide aggregate size (no. of peptides)	6.59	−3.76	11.59
H-bonded peptide pairs (no. of peptide pairs)	23.49	−2.13	6.76
stacked peptide pairs (no. of peptide pairs)	22.26	−0.86	2.78
first water shell (no. of water molecules)	8.39	224.79	384.04
second water shell (no. of water molecules)	7.77	468.16	666.99
apolar−apolar contacts (no. of atom pairs)	9.94	−1502.37	4090.68
polar−polar contacts (no. of atom pairs)	11.31	−267.37	916.66
main-chain H-bonds (no. of H-bonds)	16.07	−18.65	52.23
peptide energy (kcal/mol)	18.52	−160.88	−167.98

[a] All curves are fitted by $A^*\exp(-t/T) + B$.

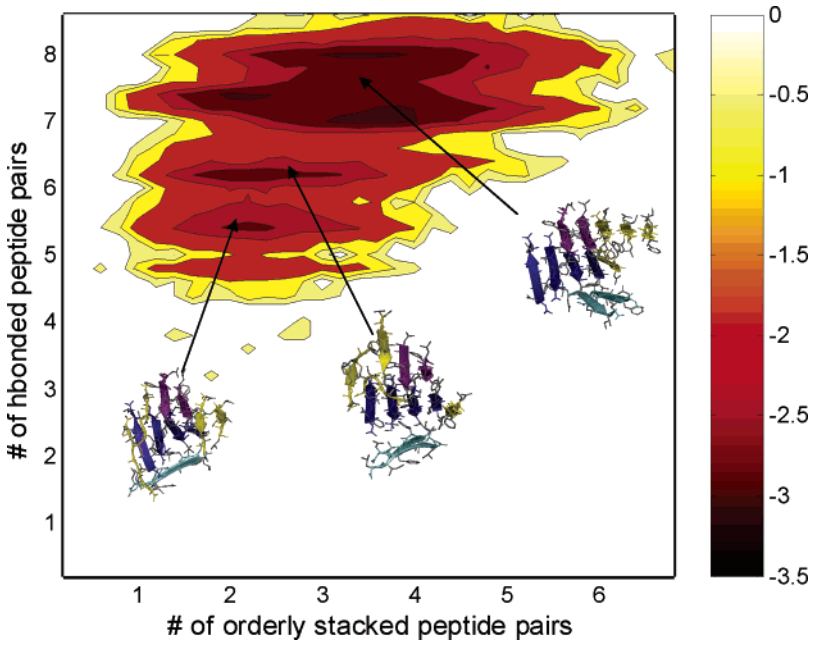

Figure 4. Two-dimensional potential of mean force calculated from the last 50.0 ns of the simulations. $\Delta G_n = -RT \ln P_n$ in kcal/mol, where T is the temperature, and P_n is the population. The representative structures of the main basins are shown. Based on the two order scores, the order space was divided into discrete grids with length 0.2. The horizontal axis is the number of peptides along the β-sheet hydrogen-bond direction, and the vertical axis is the stacked β-sheets.

the ordered peptide aggregate already passed the initiation process and has become stable at its present size.

Desolvation is an important part of aggregation process. This is illustrated by the reduction of water molecules in the solvation shells (Figure 3B). The peptide system lost about 40% of the first two solvation shells during the process; the first solvation shell dropped to 378 from initially 600, and the second shell dropped to 660 from initially 1130. The effect is even more dramatic if one considers that most of the reduction of solvation shells was due to desolvation of four peptide monomers because the initial ordered peptide aggregate was well ordered and was less solvated than the peptide monomers. Evidentially, this suggests a strongly favorable entropic contribution by releasing water molecules into the bulk solvent. It also appears that the desolvation took place in a rather early phase during which the peptide monomers collapsed to the initial ordered peptide aggregate. The time constants of water release were about 7.8−8.4 ns, close to the time scale of peptide aggregate formation (6.6 ns).

Among the atomic contacts, contacts between apolar atoms formed slightly faster than both polar−polar and hydrogen-bond contacts. The apolar−apolar atomic contacts formed at a time constant of 9.9 ns, the polar−polar contacts were 11.3 ns, and the hydrogen bonds were 16.1 ns (Figure 3C and Table 1). The sequence of these events is consistent with the notion that hydrophobic collapse took place first, followed by ordered formation of main-chain hydrogen bonds. The relatively small difference between these time constants is due to the fact that formations of these contacts were correlated.

Shown in Figure 3D is the total energy of the peptides (excluding the energies of water−water and water−peptide interactions). The curve was fitted by a single-exponential function, and the parameters are given in the Table 1. Overall, the peptide energy decreased by more than 160 kcal/mol. This was in sharp contrast to the rather mild reduction of total energy of the entire system. The total energy of the system was rather noisy because of the system size (a total of 22 419 atoms), and the root-mean-square fluctuation of the total energy was 25.3 kcal/mol when averaged over 10 simulations. Despite the large fluctuation, the total energy remained essentially flat with a slight reduction by about 10 kcal/mol when averaged over the first and last nanoseconds. This was much smaller than the 160 kcal/mol drop in the peptide energy. Because the relatively small changes in total energy and large change in peptide energy, the solvation energy (or the energy component of solvation free energy) actually increased during the simulations, mainly because of the increase in the interaction energies between the peptides and water. This, of course, did not count the favorable entropic contribution from releasing water into the bulk solvent. Nevertheless, it became clear that peptide interaction was much more favorable than the solvation energies. This was because the peptide monomers were well solvated in water before they formed aggregate and their main-chain peptide atoms formed good hydrogen bonds with water; desolvation effectively removed these favorable interactions. This term compensated almost completely the very favorable energy term of peptide−peptide interactions. When favorable water−water interactions are taken into account, the total potential energy of the system becomes weakly favorable toward the aggregation. The large favorable peptide−peptide energy also indicates the role of main-chain hydrogen bonds, which played important roles in directing formation of the ordered peptide aggregate.

The potential of mean force was constructed from the last 50 ns simulations using the number of hydrogen-bonded peptide pairs (horizontal x-axis) and the number of stacked peptide pairs (vertical y-axis) as the reaction coordinates and is shown in Figure 4. There are three distinctive minimum basins on the free-energy surface at, respectively, ($x = 2.4$, $y = 5.4$), ($x = 2.5$, $y = 6.2$), and ($x = 3.5$, $y = 7.5$), separated by two barriers. The representative structures are also shown in the figure. The

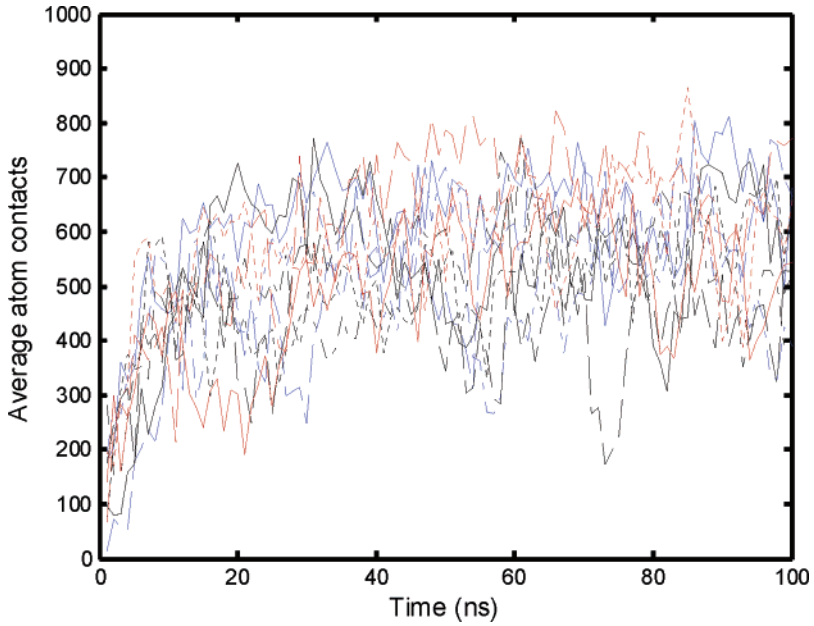

Figure 5. Average number of atom contacts (per peptide) between monomer peptides and the octamer oligomer.

basin at ($x = 3.5$, $y = 7.5$) was the most populated state with highest structural order and well-formed β-sheets. In comparison, the other two basins were less populated and structured. The least populated state, ($x = 2.4$, $y = 5.4$), was also the least ordered state among the three states. This state, in which the newly added peptides were mostly disordered and which has the highest peptide entropy, provides the entry point on the free-energy landscape, which funneled the system toward the well-ordered peptide aggregate. The state at ($x = 2.5$, $y = 6.2$) is adjacent to both the least and the most ordered states and is separated from them by barriers of about 1.0 kcal/mol. Because its stability is also between the other two states, it effectively plays a role to bridge the other two states and helps to funnel the peptide system to the ordered product state.

A set of 10 complementary simulations was conducted without the peptide backbone conformational restraints. Similar to the restrained simulations, four peptide monomers were added to a preformed ordered peptide aggregate in a box of water. By the end of the 100 ns simulations, most free monomers attached to the initial octamer. The aggregate grew by a first ordered kinetics with a time constant of 10.9 ns (or 1.3×10^{11} M^{-1} s^{-1}), comparable to the rate observed in the restrained simulations (6.6 ns or 2.1×10^{11} M^{-1} s^{-1}). As one may expect, the conformational restraints did not have a significant effect on the initial collapse process, perhaps because it was mainly driven by desolvation.

Shown in Figure 5 are the average number of atom contacts per peptide between the monomeric peptides and the octamer. After the initial growth of the atom contacts, which indicated a growth of the oligomer size, the number of atom contacts fluctuated between 300 and 800 after 20.0 ns. This large degree of fluctuation is an indication of a highly dynamic process in which the peptides constantly associate with and dissociate from the oligomer.

Despite the rapid growth of the oligomer, unlike the restrained simulations, only the initial octamer nucleus remained in the ordered form throughout the unrestrained simulations (data not shown) and newly attached peptides were disordered. Thus, the growth mode was disordered and amorphous in this set of simulations at this stage.

Discussion

Our previous two studies focused on the initiation of the ordered peptide aggregates. The first study showed that the formation of the initial (mostly disordered) peptide oligomers was mainly driven by hydrophobic interaction and the dissociation of the disordered aggregates might be the rate-limiting step for the formation of ordered oligomers.[37] In the second study, we showed that the nucleation process appeared to obey the second-order kinetics and a large fraction of the products was disordered.[38] Therefore, the dissociation of the disordered oligomers was necessary to form ordered peptide oligomers. In this study, we focused on the elongation process of the ordered peptide aggregate. When the peptides were restrained to the extended conformation, the elongation process was dominated by ordered growth in which the peptides were attached to the ordered peptide aggregate initially in disordered orientation and moved to the ordered orientation upon formation of main-chain hydrogen bonds with the ordered oligomer.

We calculated the key structural parameters of the final ordered peptide aggregate. The calculated inter-strand distance of the β-sheets was 4.5 ± 0.4 Å, which is compared to the 4.60 and 4.83 Å observed in the X-ray fiber diffraction experiments of a similar peptide.[8] The interlayer distance of the peptide NFGAIL was 8.5 ± 0.6 and 7.7 ± 1.1Å for, respectively, the parallel and antiparallel β-sheet stacking. These distances agreed qualitatively with the major distance 8.60 Å obtained from the fiber diffraction data of the decapeptide SNNFGAILSS.[8]

Among the ordered peptide aggregates, fluctuation of the inter-strand spacing within the same β-sheet was quite small with a root-mean-square fluctuation of about 0.4 Å, considerably smaller than the interlayer spacing fluctuation of 1.1 Å. This indicated side-to-side association through β-sheet hydrogen bonds was more stable than stacking and reinforced the notion that the main-chain hydrogen bonds played a major role in determining the ordered oligomer structures.

Consistent with our earlier observation, we did not observe significant preference of forming either parallel or antiparallel β-sheets. Within the last snapshots of the simulations (Figure 1), there were 16 parallel β-sheet extensions and 14 antiparallel extensions. Thus, the preference at this stage appears to be weak, which is consistent with the observations made on other peptides[28] in which small fragments were found to prefer antiparallel β-sheets by about 20%. In our case, most of the ordered peptide aggregates observed in the simulations comprised mixed parallel and antiparallel β-sheets. Naturally, one may still ask whether any preference will be developed at even a later stage. Our simulations indicated that this may not be the case because the simulations have already extended into the elongation stage. Therefore, our simulations suggested that the preference of NFGAIL peptide is inherently weak throughout all three stages we have studied so far, including the aggregation stage in which peptides form disordered aggregates,[37] the initiation stage in which small ordered aggregates start to form,[38] and the elongation stage when the ordered peptide aggregate starts to grow. However, given the limited number of transitions between antiparallel and parallel alignments, quantitative characterization of the preference is not warranted.

The dynamic nature of the aggregation process has been somewhat under appreciated. Efforts in the past have more or less focused on the structural features of the fibrils. With the increased knowledge on the super structures of amyloid fibrils and growing evidence of the toxicity of early species, the community shows increasing interest in the formation of some of the early low-weight oligomers and initiation of ordered aggregates. In the two sets of simulations reported here and those reported earlier, we observed a rather dynamic process in which peptides undergo constant association and dissociation. In our view, this is necessary for the conformational transition. Nevertheless, our simulations do not support the notion that the primary pathway of amyloid formation is through spontaneous conformational transitions of amorphous aggregates to ordered form.

In this study, we chose to use explicit model to represent the solvent. In comparison to continuum solvent models, the presence of a large number of water molecules makes the simulations expensive due to both the cost to evaluate energy and the solvent viscosity. In the past, many investigators have applied continuum solvent and other simplified models to study similar systems. In our group, we also applied Generalized Born in the studies of peptide and protein folding. While the development of continuum solvent and other simplified models is quite encouraging and excellent results have been obtained, explicit models have a unique advantage to model the molecular level interactions between solvent and peptides. For example, explicit solvent models have been calibrated to model hydrogen-bond interactions, which play important roles in amyloid fibril elongation.

We shall also note the inherent sampling difficulty in this type of simulation. Due to the detailed model and associated computational cost, simulation at the scale reported here is still a challenging endeavor. Despite the extensive simulation, sampling is quite limited. A direct consequence of the limited sampling is that the conclusions are typically qualitative. In this study, we chose to use multiple simulations, which allowed us to examine the level of consistency between the simulations. As demonstrated from the simulations, although different by detail, many of the events were observed in multiple simulation trajectories, suggesting that these were the preferred pathways and that the simulations were consistent with one another. Indeed, our conclusions and discussions have been based on these consistent events.

Conclusion

In this study, the elongation of ordered peptide aggregate was modeled by placing four peptide monomers into a solution where a well-ordered octamer from our previous study was used as a nucleus. In one set of 10 simulations, the peptides were restrained to the β-extended conformations. An ordered growth of a peptide oligomer was observed that obeyed the first-order kinetics. The main growth mode was the elongation along the β-sheet hydrogen-bond direction. The primary pathway is a two-stage process where the peptides initially aggregated to the ordered peptide aggregate and subsequently moved to the ends of the β-sheets where the peptides form stable hydrogen bonds with the β-sheets. A secondary pathway was also observed in which peptide monomers formed two-strand β-sheets, which then attached to the ordered peptide aggregate and elongated the β-sheets. The growth of the peptide aggregate was correlated with the apolar−apolar atom contacts and the reduction of water molecules in the primary solvation shell of the peptides, suggesting that the initial attachment of the free peptides to the ordered peptide aggregate was driven by hydrophobic interactions. In contrast, the ordered peptide aggregate growth was correlated with the formation of hydrogen bonds, which was the main driving force of β-sheet elongation. Within the context of the present and our earlier studies on NFGAIL peptide, we observed almost equal tendency to form parallel and antiparallel β-sheets when peptides are restrained to the extended conformation.

Different growth mode was observed when peptide conformation restraints were removed in the second set of simulations in comparison to the restrained simulation results. Most attachments in the unrestrained simulations were disordered, and the peptide conformations were heterogeneous. Nevertheless, a fast growth of the peptide aggregate was also observed, much like the fast growth in the restrained simulations, indicating that the aggregation was independent of peptide conformation and mainly driven by hydrophobic interactions.

Acknowledgment. This work was supported by research grants from NIH (GM64458 and GM67168 to Y.D.).

Supporting Information Available: (1) Complete ref 39. (2) A movie clip of the representative trajectory discussed in the text. (3) Description of analysis protocol. This material is available free of charge via the Internet at http://pubs.acs.org.

JA050767X